Journal of Fibers and Polymer Composites 2 (2): 111-129 (2023)

Journal of Fibers and Polymer Composites

https://journals.gesociety.org/index.php/jfpc/index

SYNTHESIS AND CHARACTERIZATION OF PES/PEG/PVA/SiO_2 NANOCOMPOSITE ULTRAFILTRATION MEMBRANE

Silvia Widiyanti[1], Mita Nurhayati[1,2], Hendrawan Hendrawan[1], Boon Seng Ooi[3], Fitri Khoerunnisa*[1],

[1]Department of Chemistry, Indonesia University of Education, Bandung 40154, Indonesia
[2]Department of Advanced Science and Technology Convergence, Kyungpook National University, 2559 Gyeongsang-daero, Sangju-si 37224, South Korea
[3]School of Chemical Engineering, Engineering Campus, Universiti Sains Malaysia, Seri Ampangan, 14300, Nibong, Malaysia

*Corresponding author
Email: fitri@upi.edu

Abstract. *This study aims to synthesis and characterize PES/PEG/PVA/SiO_2 composite membranes. The composite membranes were synthesized by phase inversion method with composition (% w/w) Polyethersulfone/ PES (17.25), Polyvinylalcohol/ PVA (3.58; 0.85; 1.43; 2.57; 3.57, Polyethylene glycol/ PEG (3.72), Silica/SiO_2 (0.35; 0.85; 1.43; 2.57; 3.57), and Dimethyl acetamide/DMAc solvent. Composite membranes were characterized using FTIR spectroscopy, X-ray diffraction, Scanning Electron Microscopy (SEM), and water contact angle. The results showed that the interaction between PES, PVA, and SiO_2 was indicated by a shift in the typical absorption spectrum of the FTIR. SEM cross-sectional photos showed that the addition of PVA and SiO_2 caused significant changes in the morphology and pore structure of the PES membrane. The results of the X-ray diffractogram (X-Ray) showed a shift in the typical diffraction peaks of PES, PEG, PVA and the presence of new diffraction peaks of SiO_2. The crystallinity of the membrane increased from 34.99% to 57.25% which indicated that the composite membrane was successfully synthesized. The addition of PEG/PVA/SiO_2 also increased the hydrophilicity of the composite membrane. Based on these findings, it can be concluded that the PES/PEG/PVA/SiO_2 composite membrane has been synthesized through the phase inversion method with the optimum composition of PES: PEG: PVA: SiO_2 was 17.25%: 3.72%: 0.85%: 0.35%, respectively. The addition of PEG/PVA/SiO_2 increased the hydrophilicity and modified the morphological structure of the PES membrane.*
Keywords: *Characterization; Composite membrane; PES/PEG/PVA/SiO_2; Synthesis*

1. Introduction

Access to clean water is fundamental for sustaining life on earth. However, contemporary life styles coupled with increased material consumption, have led to the generation of vast volumes of wastewater, exacerbating water pollution in existing sources [1]. To address these environmental challenges, membrane technology has emerged as a promising method for water separation and purification [2]. Unlike traditional phase equilibrium-based separation processes, membrane-based separations consume significantly less energy. Moreover, the simplicity, compactness, and ease of operation make them an attractive solution, requiring

Received August 23, 2023; Accepted October 26, 2023; Published October 30, 2023
https://doi.org/ 10.55043/jfpc.v2i2.120

minimal additional equipment [3].

To date, the water purification plants have applied numerous membrane filtration methods such as microfiltration (MF), reverse osmosis (RO), nanofiltration (NF) and ultrafiltration (UF). Ultrafiltration is a pressure driven membrane separation technology. In ultrafiltration method of water purification, membrane having pore size (2–100 nm) and ~ molecular weight cut off/ MWCO (5–500 kDa), is used at operating pressure of 2–8 bar. Ultrafiltration can be an appropriate method to eliminate the impurities from water at a fairly reduced cost in comparison to other filtration methods such as reverse osmosis and nanofiltration. In addition, this method receives careful attention in the wastewater treatment, and very efficient in term of performance and consumption of energy among various filtration techniques based on membranes [4].

The growing interest in water separation technologies has spurred the development of various membranes using both inorganic and polymeric materials [5]. Polymers with moderate hydrophilicity, such as polysulfone (PS)/polyether sulfone (PES), polyacrylonitrile (PAN), and polyvinylidene fluoride (PVDF) have been widely used as membrane materials [1]. PES, in particular, stands out due to its excellence thermal, mechanical, and chemical resistance properties, along with high transition glass (Tg) values. These factors encourage the widespread utilization of PES for the membranes production with different pore sizes. However, due to its high hydrophobicity, PES membranes are susceptible to fouling [6]. To overcome this limitation, numerous methods have been introduced to modify the properties of PES membranes, including surface coating, mixing, and chemical treatment [7].

One promising approach to improve the performance of PES membranes in the filtration processes, particularly in terms of water flux, hydrophilicity and anti-fouling properties, is by means of incorporation of hydrophilic additives. Polyvinyl alcohol (PVA), for instance, exhibits the ability to change its nature from hydrophobic to hydrophilic [8]. Despite being a water-soluble biodegradable polymer, PVA's swelling behavior in liquid media can impact membrane rejection performance [9]. Similarly, polyethylene glycol (PEG) can be utilized as an additive, contributing to the formation of macrovoids in the membrane sublayer, leading to increased pure water flux and Bovine Serum Albumin (BSA) rejection [10].

In addition, incorporating nanomaterials into the PES membrane can significantly improve their mechanical properties. Silicon dioxide (SiO_2) nanoparticles is commonly used to synthesize the composite membranes for filtration applications, possess a good porous structure and –OH groups that enhance the membrane hydrophilicity and surface properties.

Additionally, the inclusion of SiO_2 facilitates water diffusion into the membrane, resulting in elevated solute rejection and enhanced fouling control [11].

Considering the great potential of incorporating PVA and SiO_2 into PES membranes, this research aims to synthesize and characterize PES composite membranes with the inclusion of PVA, PEG, and SiO_2. Specifically, the study systematically investigates the impact of PEG/PVA/SiO_2 addition on the chemical and physical properties of PES membranes. By understanding the effects of these additives, this research seeks to contribute to the development of advanced nanocomposite membranes for efficient water purification applications.

2. Methods

2.1. Material

In this study, PES (58 kDa) was used, sodium metasilicate, DMAc (purity of > 99.5%), PEG (6 kDa), PVA (13 kDa, degree of hydrolysis 97%), ammonia, ethanol, nitric acid and deionized water. All chemicals used in this study were pro analysis grade and purchased from Merck Germany.

2.2. Methods

The process flowchart of this research was depicted in Figure 1. Mainly, this work consists of synthesis and the characterization processes. The data obtained from characterization were analyzed to come to the conclusion. Detailed description of each process is described in the respective section below.

2.2.1. Synthesis of composite membranes

The synthesis process was shown in Figure 2. SiO_2 nanoparticles were prepared by dissolving 3.6 grams of sodium metasilicate in 100 mL of deionized water. This solution was slowly added drop by drop into a solvent mixture containing 120 mL of ammonia-ethanol (3:1) and left to stand for one hour. A 5% PVA solution was prepared by dissolving 5 grams of PVA in 100 mL of water. The solution was then heated to 90^{o}C. The SiO_2 nanoparticles solution was adjusted to pH=3 using nitric acid. Subsequently, the solution was mixed with the previous PVA solution at a ratio of PVA:SiO_2 = 5:2. The mixing process was carried out for 4 hours at 90°C to obtain a homogeneous casting solution.

PES/PEG/PVA/SiO_2 membranes were synthesized through Non-solvent Induced Phase Inversion (NIPS) with specific composition ratios, as outlined in Table 1 in the total volume of casting solution of 100 mL. In this method, a polymer solution film is immersed in a nonsolvent bath, inducing phase separation of the film into a polymer-rich phase that becomes the membrane matrix and a polymer-poor phase that becomes the membrane pores [12]. It starts

with a spontaneous change in the chemical potential of the polymeric substance, causing movement of the polymer towards the film interface. This increases the polymer concentration at the interface until it becomes rigid and forms a skin layer, which prevents further transportation of the non-solvent into the film [13]. The mixture was then stirred using a mechanical stirrer at 500 rpm and a temperature of 80^{o}C. Membrane was casted by pouring 10 ml of liquid into a plate sized 12 cm x 10 cm and then immerse in a water bath for 24 hours. After that membrane was dried in desiccator for 24 hours.

Table 1. The composition ratio of PES/PEG/PVA/SiO_2 composite membranes

Membrane	Composition (% w/w)				
	Precursors			Porogen	solvent
	PES	PVA	SiO_2	PEG	DMAc
P	18	-	-	-	82
MPS-0	17.25	3.58	-	3.72	75.45
MPS-1		0.85	0.35		77.83
MPS-2		1.43	0.57		77.03
MPS-3		2.57	1.03		75.43
MPS-4		357	1.43		74.03

2.2.2. Characterization

To assess the membrane thickness, measurements were taken at 4 different points using a digital screw micrometer (Mitutoyo 0-25mm ± 0.0001 mm). The average value of the measurements was calculated, and the average membrane thickness was obtained for the various PVA/SiO_2 compositions. The structure and functional groups of the membrane were analyzed using FTIR (FTIR-Shimadzu 4800, using KBr pellets with scanning rate 0.02 cm^{-1}/s). The membrane crystal structure was analyzed using X-ray diffraction machine (XRD Bruker D8 Advance, 3 kW) with X-ray resource CuKα (1.54060 Angstrom) and 2θ 5-60^{o}. The morphology of the membranes were characterized through Scanning Electron microscope (SEM JEOL/JMS IT300 LV, Coating SEM DII-29030SCTR, 15 kV). Meanwhile, to determine the surface hydrophilicity of the membrane, the measurements were carried out through sessile drop method, by dripping 20 µL of deionized water and measuring the contact angle between the distilled water and the membrane surface through the drop snake feature in the ImageJ software.

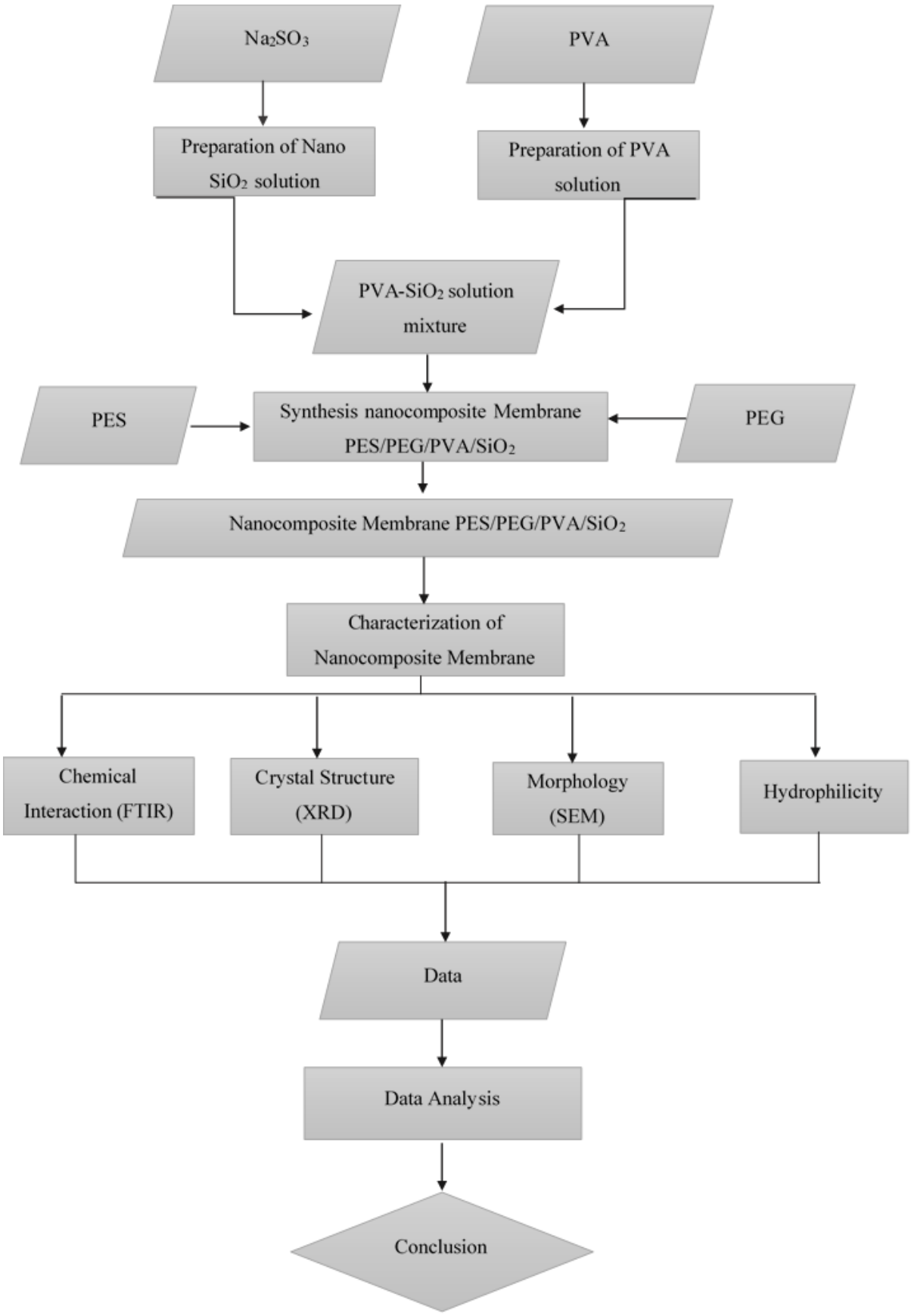

Figure 1. Process flowchart of nanocomposite membrane development

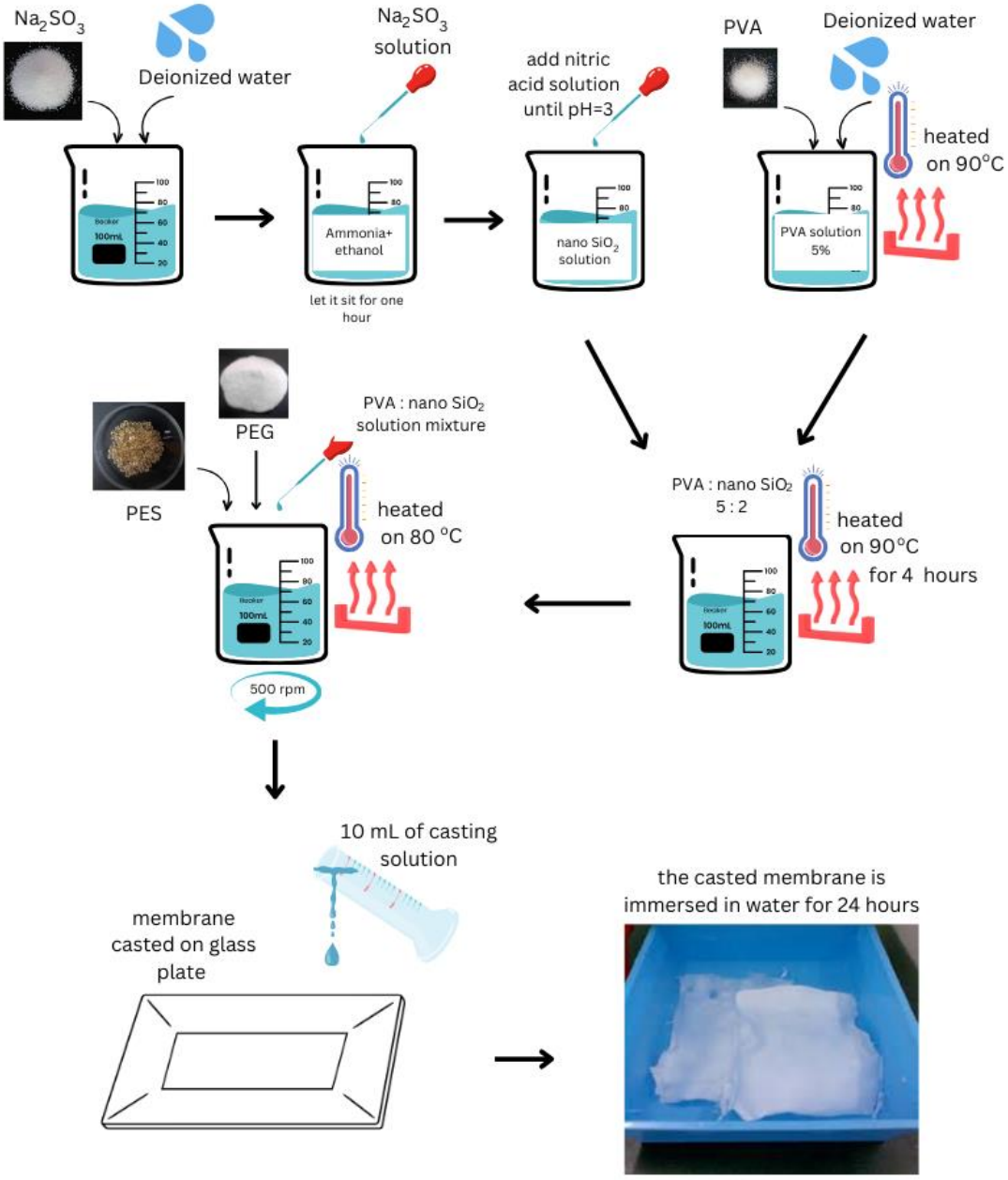

Figure 2. Synthesis of PES/PEG/PVA/SiO_2 Nanocomposite Membrane

3. Results and Discussion

The PES/PEG/PVA/SiO_2 composite membrane was successfully synthesized, exhibiting a uniform white physical appearance. Notably, all the synthesized membranes displayed consistent coloration, indicating homogeneous dispersion of the membrane precursors throughout the matrix. Figure 3 shows a visual representation of the synthesized membrane. Each membrane is denoted based on its respective PVA/SiO_2 composition. Specifically, the PES membrane was labeled as P, while the PES/PEG/PVA composite membrane was labeled as MPS-0. The PES/PEG/PVA/SiO_2 composite membranes are labeled MPS-1, 2, 3 and 4, corresponding to the compositions specified in the Table 1. The thickness variations among the PES/PEG/PVA/SiO_2 composite membranes were presented in Figure 4.

3.1. Chemical Interactions Between Membrane Precursors

Chemical interactions in the PES/PEG/PVA and PES/PEG/PVA/SiO_2 composite membranes were analyzed using FTIR instruments, and the corresponding spectra are depicted in Figure 5. Figure 5(A) represents the composite membrane spectra, while the specific absorption band from 1800-530 cm^{-1} is highlighted in Figure 5(B). Notable shifts in the peak within the absorption band 1292 cm^{-1} to 1315 cm^{-1} and from 1151 cm^{-1} to 1154 cm^{-1} were observed, indicating asymmetric vibrational interactions of the O=S=O functional group [14]. In addition, in MPS-1, 2, 3, 4, a new peak emerged, absent in both P and MPS-0. This peak appeared in the absorption band at 954 cm^{-1} and shifted with an increasing PVA-SiO_2 content, indicating Si-OH interactions [15].

Furthermore, peak broadening occurred in the absorption bands at 1482 and 1577 cm^{-1}, indicating aromatic C-H interactions [14, 16]. Interactions involving C-O-C were evident at 1243 cm^{-1} [14], and -OH bending interactions were observed at 1407 cm^{-1}. These findings provide compelling evidence of interactions between PES, PEG, PVA, and SiO_2, which likely occur through hydrogen bonds and van der Waals interactions. Table 2 represents information on the absorption peaks of the FTIR spectra of the composite membrane.

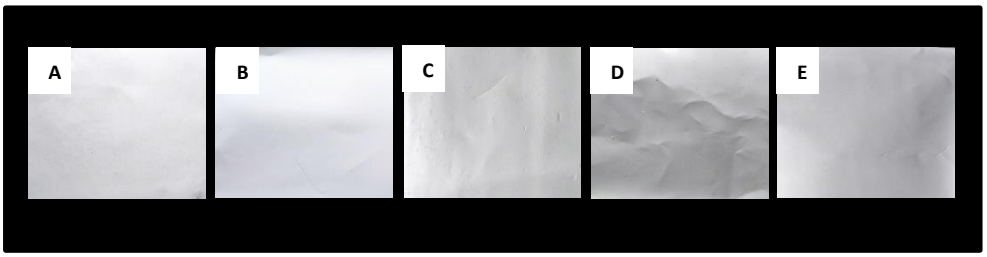

Figure 3. The PES/PEG/PVA/SiO_2 Nanocomposite Membranes Photograph. (A) MPS-0, (B) MPS-1, (C) MPS-2, (D) MPS-3 and (E) MPS-4

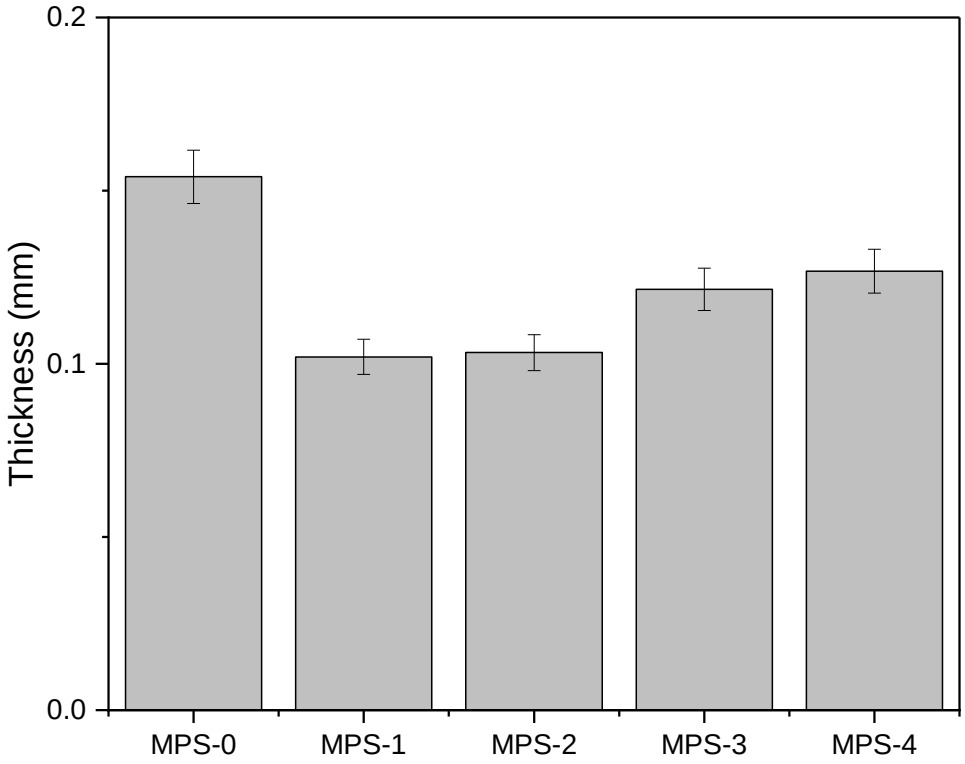

Figure 4. The thickness of nanocomposite membranes

The FTIR analysis of the MPS-0 spectrum revealed an absorption peak at 3442 cm^{-1}, indicating an interaction between the -OH groups present in the PEG and PVA compounds [17]. The -OH vibration absorption shifted after the incorporation of PVA/SiO_2 into the composite membrane, resulting in wavenumbers of 3442 cm^{-1} to 3436, 3449 and 3455 cm^{-1}. Similarly, the C-H vibrations absorption also experienced shifts from 2927 cm^{-1} to 2862, 2865 and 2868 cm^{-1}, as a consequence of variations in the PVA/SiO_2 composition within the composite membrane [18].

Figure 6 illustrates the interactions occurring in the composite membrane precursor refer to the FTIR results. The figure represented the interaction between Si-OH and -OH from PVA interaction. Furthermore, the observed shift in the -OH peak, though not significant, indicates additional Van der Waals interactions between PVA and silica molecules. In addition, the significant shift in the S=O vibration can be attributed to interactions with the hydrogen bonding to -OH in PVA. This interaction further confirms the trapping of PVA/SiO_2 within the polymer matrix, signifying the successful synthesis of the composite membranes.

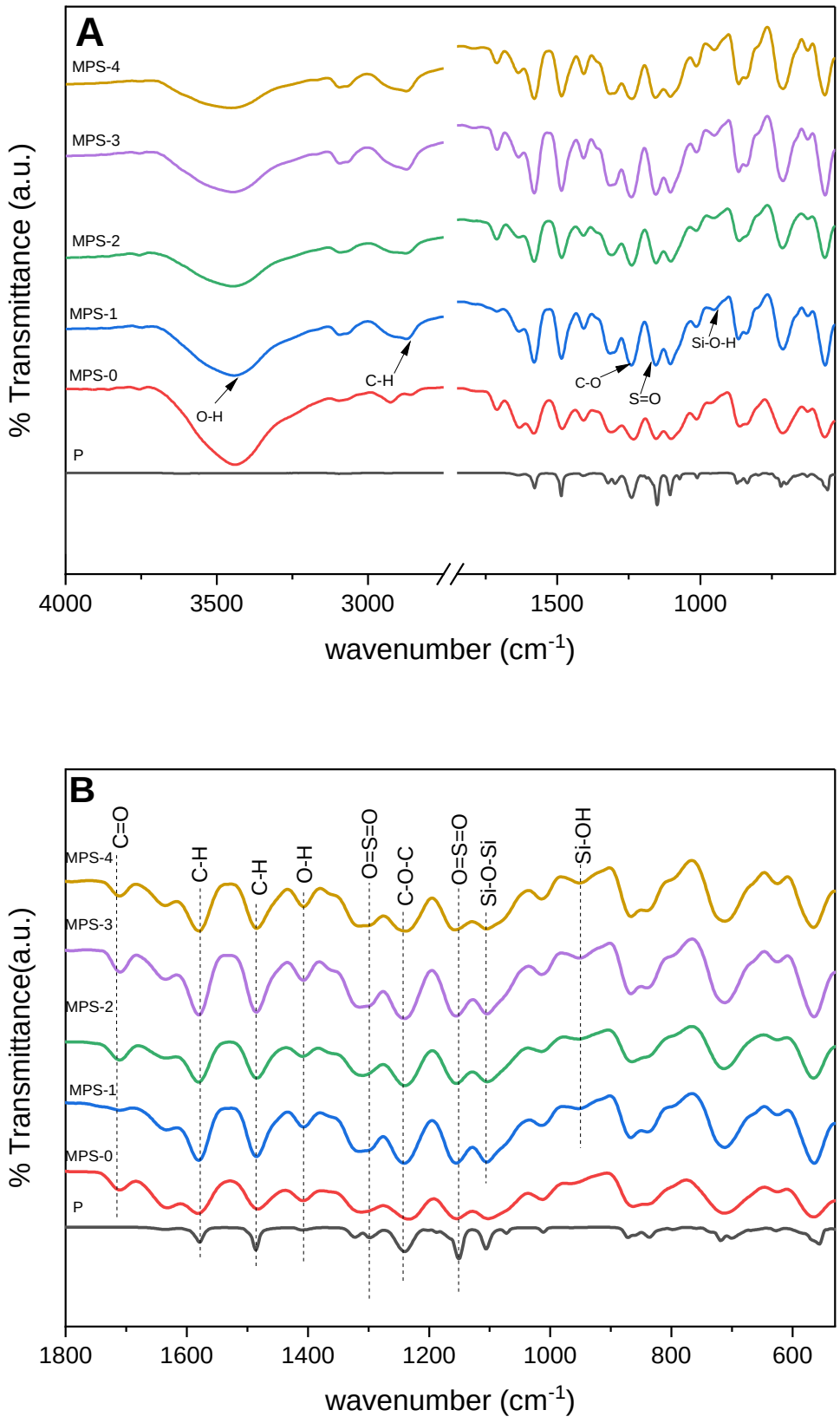

Figure 5. (A) FTIR spectra of nanocomposite membranes and (B) magnified FTIR spectra at wavenumber range of 1800-530 cm^{-1}

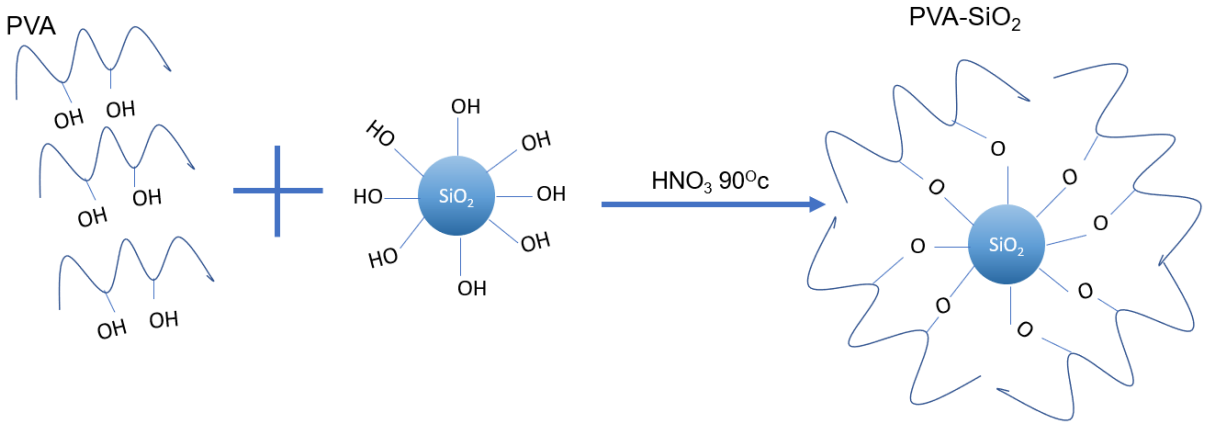

Figure 6. Chemical interaction between PVA and SiO_2

Table 2. FTIR absorption peaks of the composite membranes

Group	Wavenumber (cm^{-1})						Vibration modes	References
	P	MPS-0	MPS-1	MPS-2	MPS-3	MPS-4		
Si-OH	-	-	954	948	944	944	Asymmetrical vibration	[36]
Si-O-Si	-	-	1104	1102	1105	1108	Asymmetrical vibration	[37]
O-H	-	3442	3436	3449	3455	3455	stretching	[38]
O=S=O	1151	1154	1157	1154	1157	1157	Symmetrical vibration	[39]
O=S=O	1292	1315	1318	1312	1315	1315	Asymmetrical vibration	[14]
C-H	-	2927	2862	2865	2868	2868	stretching	
C-H benzene	1482	1482	1482	1482	1482	1482	stretching	[16, 39]
C-H benzene	1577	1577	1577	1577	1577	1577	vibration	[16]
C-O-C	1243	1243	1243	1243	1243	1243	stretching	
O-H	-	1407	1407	1407	1407	1407	bending	[40]

3.2. Membrane Structure and Morphology

The morphological structure of the PES/PEG/PVA/SiO_2 composite membrane was examined through cross-sectional SEM, as depicted in Figure 7 at 250x and 10000x magnification. Prior to modification, the PES membrane exhibited a porous structure. However, in the MPS-0 composite membrane, the asymmetrical pore structure disappeared, and irregularly distributed macrovoids were formed. This phenomenon could be attributed to the PVA and PEG addition to the casting solution. PVA and PEG are hydrophilic nature, which means when phase inversion occurred, the water come in faster than the organic solvent come out [19]. The addition of PVA/SiO_2 induced the formation of asymmetrical structure that connect the upper and lower pores. This increased connectivity between the upper lower pores structure can increase permeability

[20]. Higher incorporation of PVA/SiO_2 resulted the denser structure however, the connectivity of the upper with lower pore structures decreases. Interestingly, the cross-sectional images did not show any agglomeration of SiO_2 nanoparticles, and at 10000x magnification, it became apparent that the addition of PVA/SiO_2 led to the more evenly sized pore structure.

The formation of finger-type structures occurred in two stages: initiation and propagation. Initiation stage occurred at points where the skin layer broke due to stress shrinkage and syneresis. Subsequently, radius growth occurred at this break points, propagating to the bottom of the polymer film. The continuous mixing process caused the separation of polymer solution into a polymeric substance-rich phase, creating the membrane structure, and the non-polymer phase, forming the membrane pores. The internal structure demonstrated a hierarchical arrangement with a solid shell layer at the solvent/non-solvent interface [21].

According to the Mckelvey and Koros hypothesis, macrovoid formation began with nucleation of the polymer phase just below the skin layer, and its growth was influenced by the rate difference between the diffusion of the nonsolvent into the casting solution and the solvent into the coagulation bath. This rate difference induces a nonsolvent concentration gradient in the casting solution, which is the driving force for macrovoids growth. The viscosity of the casting solution increased with the addition of SiO_2 that will slow down the gelation of the PES membrane. This slowed down nonsolvent diffusion and led to a decrease in nonsolvent concentration, inhibiting the formation or growth of macrovoids in the membrane [20].

The surface SEM images of the composite membranes are presented in Figure 8. MPS-0 showed macropores on the surface, and upon detailed observation, a spongy-like structure representing the underlying pore structure was visible. However, the pore structure on the surface is reduced and denser. As PVA/SiO_2 (MPS-1) is added, the membrane surface becomes denser and will hinder achieving maximum permeability and selectivity with minimal transport resistance [22]. Therefore, MPS-1 exhibited the most favorable structure with more evenly distributed macrovoid and microvoid pore sizes and a less dense surface. This formed structure will contribute significantly to performance of the composite membranes in separation process

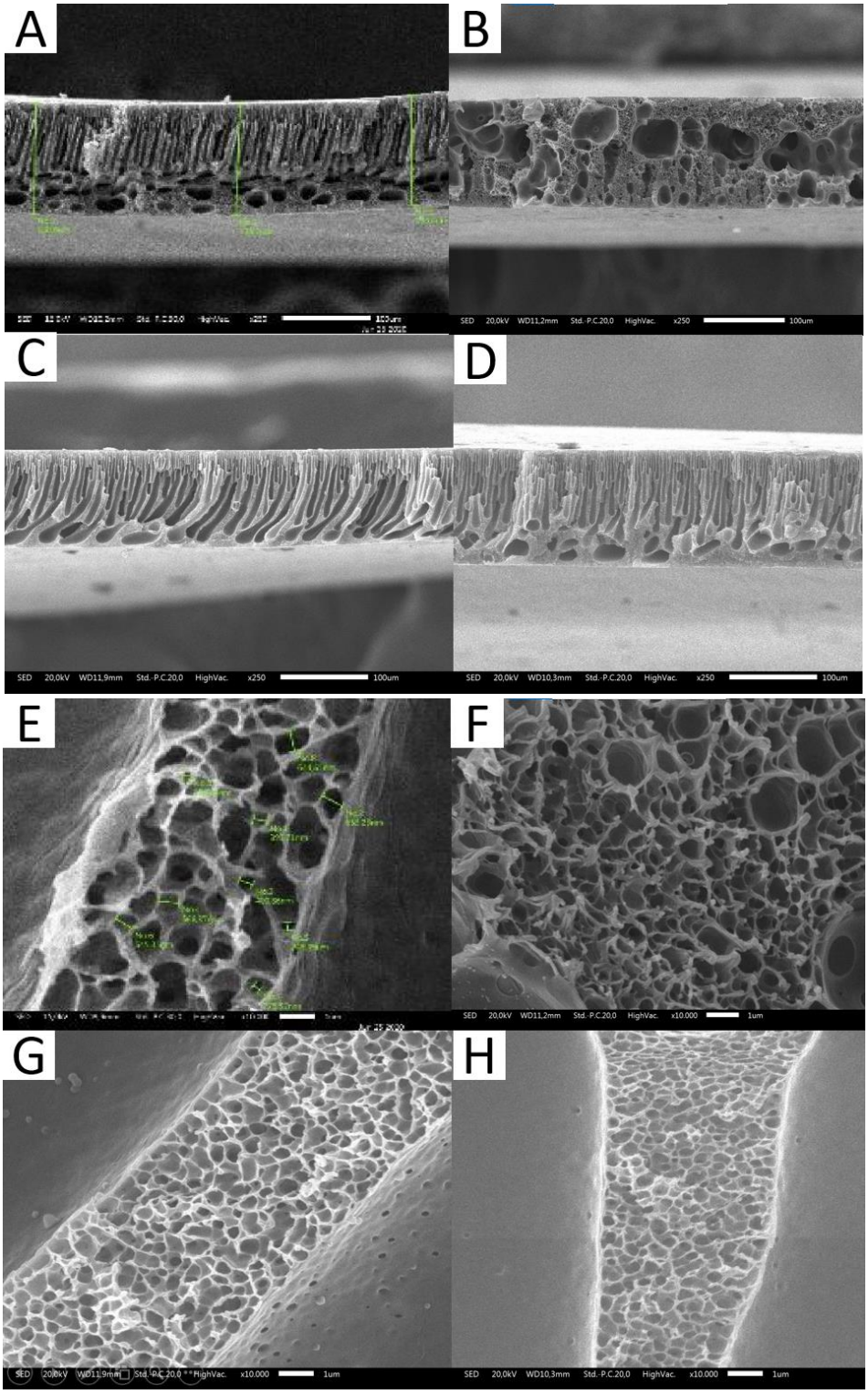

Figure 7. The cross-section SEM images of the nanocomposite membranes at 250x magnification of (A)P, (B) MPS-0, (C) MPS-1, and (D) MPS-4 and at 10000x magnification (E) P, (F)MPS-0, (G) MPS-1, (H) MPS-4

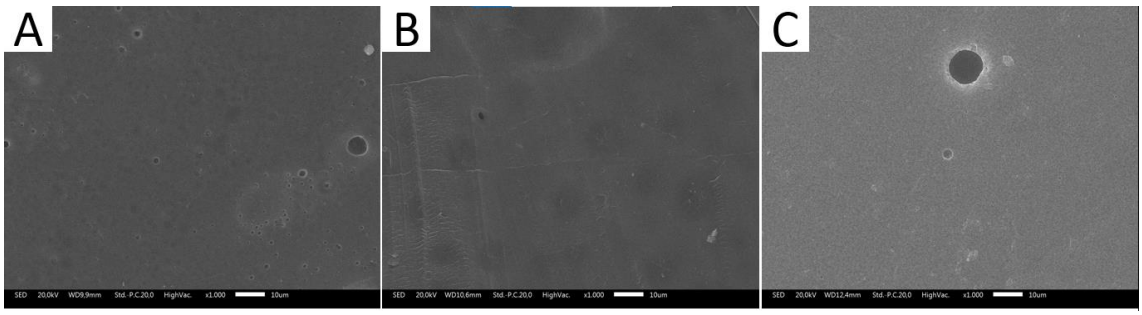

Figure 8. The surface SEM image of the composite membrane (A) MPS-0, (B) MPS-1, and (C) MPS-4.

3.2.1. Hydrophilicity

The hydrophilicity test of the membrane was carried out by measuring the water contact angle (WCA). Water contact angle is one of the mainly analyzed to determine the hydrophilicity of the membrane. Hydrophilic membranes usually exhibited WCA below 90º, with lower values indicating higher hydrophilicity [23, 24]. Hydrophilicity of the membrane depends on the composition of the substance and the corresponding membrane surface. Hydrophilic membranes are very important in water treatment application to prevent organic matter fouling on the membrane surface [23]. They also offer advantages in water filtration processes by promoting a higher permeate flux due to the low interaction between the membrane and the hydrophobic materials [25].

Figure 9 illustrates the WCA graph of the composite membrane. When PEG and PVA were added individually to the PES membrane, no significant change in WCA was observed. However, after the addition of PEG/PVA/SiO_2, the WCA value of the membrane decreased indicating an enhanced hydrophilic nature. The decrease in WCA on the PES/PEG/PVA/SiO_2 composite membrane can be attributed to the presence of –OH groups from PEG and PVA which are capable of forming hydrogen bonds. In addition, the presence of hydrophilic silica contributed to the increase of membrane hydrophilicity [20]. As the PVA/SiO_2 composition increased, the WCA value showed a tendency to rise. This can be related to the morphological structure of the membrane. At higher concentrations of PVA/SiO_2, the upper pore structure may not well connect to the lower pore structure, so that water molecules are more retained. Nonetheless, the WCA values obtained for composite membranes over the entire range of compositions were still < 90º. This shows that the PES/PEG/PVA/SiO_2 composite membrane has hydrophilic properties, so that it has the great potential to be used in filtration applications, especially in water purification.

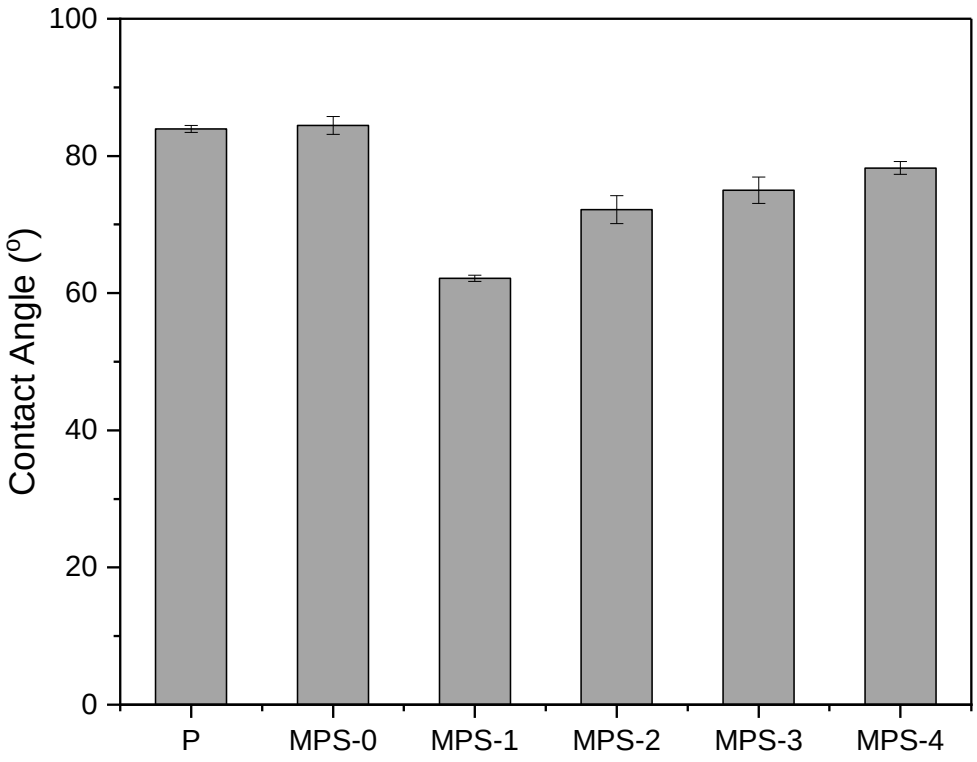

Figure 9. Water contact angle (WCA) of the nanocomposite membrane

3.2.2. Composite Membrane Structure and Crystallinity

XRD test was conducted to investigate the crystal structure of each precursor in the membrane. The X-Ray diffractogram of the composite membranes is presented in Figure 10. The typical PES diffraction peak was observed at 18.73° [26]. Following the addition of PEG/PVA, the diffraction peak of PES shifted to 18.56° with Miller indices (1 2 0) [27], indicating an alteration in the crystal lattice due to the interaction between these precursors. Diffraction peaks was found at 13.21° (1 1 1)[28] and 16.62° (2 0 2) [29], which is a typical peak for PVA [30] and 23.79° (3 1 1) [31] which is a typical peak PEG diffraction [32]. In the MPS-1 diffractogram, the diffraction peaks shifted to 14.21° and 16.97° for PVA; 25.28° for PEG; 18.73° for PES. These shifts indicated an interaction between the various precursors within the membrane matrix. In addition, at MPS-1, a new diffraction peak was found at 2θ 31.69° with Miller indices (4 1 0) [33] which indicates an amorphous phase of SiO_2 [34]. This result inferred that SiO_2 nanoparticles were successfully incorporated into the matrix of composite membrane.

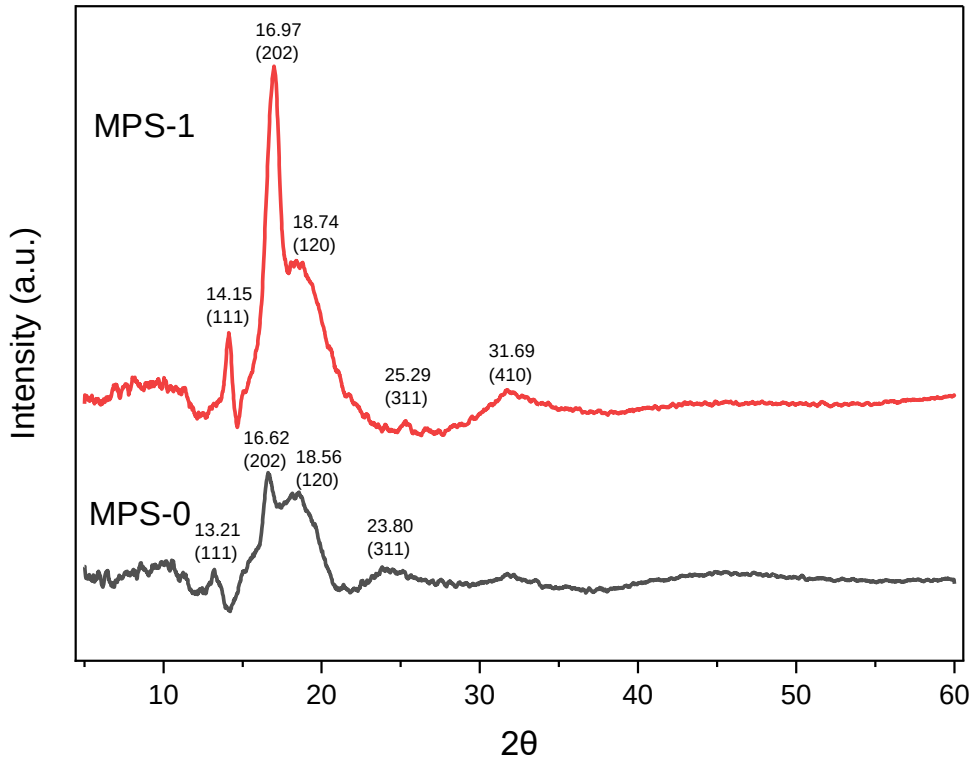

Figure 10. X-Ray diffractogram of nanocomposite membranes

The addition of SiO_2 to the composite membrane significantly increased the crystallinity of the membrane, which was indicated by the formation of sharper diffraction peaks (the smaller full width half maximum / FWHM). The crystallinity of the membrane can be measured by calculating peak area per total area. From the calculation, it is indicated that the crystallinity of membrane increased from 34.99% to 57.25%. Crystalline membranes possess an ordered structure, and the increased crystallization is expected to the enhance of the mechanical properties [35]. Therefore, it is expected that the synthesized composite membrane would exhibit favorable mechanical properties, that beneficial for the membrane-based separation process.

4. Conclusions

The PES/PEG/PVA/SiO_2 composite membrane was successfully synthesized through the NIPS method with an optimized composition of PES: PEG: PVA: SiO_2 (17.25%: 3.72%: 0.85%: 0.35%). The addition of PEG/PVA/SiO_2 modifies the characteristics of the PES membrane, where the shift in the typical FTIR absorption peak indicates an interaction between PES and PEG/PVA/SiO_2. Moreover, SEM photographs demonstrated the remarkable modification of the morphological structure of the nanocomposite membrane, indicated by the formation of macrovoids and microvoids, as well as a denser and more evenly sized membrane pore structure.

These morphological changes are crucial as they can impact the membrane's permeability and selectivity in ultrafiltration applications. The hydrophilicity test results showed an improvement in hydrophilic behavior with the addition of PEG/PVA/SiO_2 composition. It is essential for reducing fouling and enhancing water permeability during water purification processes. Furthermore, the X-ray diffractogram revealed notable changes in the morphological structure and increased crystallinity of the PES membrane after the incorporation of SiO_2. The increased crystallinity suggests an ordered structure, which may contribute to improved mechanical properties and durability of the composite membrane. Overall, the PES/PEG/PVA/SiO_2 composite membranes with enhanced morphological, hydrophilic, and crystalline characteristics offers promising properties for water purification.

Acknowledgment

We gratefully acknowledge the excellent supports provided by World Class Professor (WCP) grant (2808/E4/DT.04.03/2023); Riset Kolaborasi Indonesia (RKI) grant (961/UN40.LP/PT.01.03/2023) and UPI research grant (540/UN40.LP/PT.01.03/2023).

References

[1] T. Gullinkala and I. C. Escobar, "Membranes for Water Treatment Applications – An Overview," in *ACS Symposium Series*, vol. 1078, I. Escobar and B. Van Der Bruggen, Eds., Washington, DC: American Chemical Society, 2011, pp. 155–170. https://doi.org/10.1021/bk-2011-1078.ch010.

[2] M. Sadrzadeh and S. Bhattacharjee, "Rational design of phase inversion membranes by tailoring thermodynamics and kinetics of casting solution using polymer additives," *J. Membr. Sci.*, vol. 441, pp. 31–44, Aug. 2013, https://doi.org/10.1016/j.memsci.2013.04.009.

[3] C. A. Quist-Jensen, F. Macedonio, and E. Drioli, "Membrane technology for water production in agriculture: Desalination and wastewater reuse," *Desalination*, vol. 364, pp. 17–32, May 2015, https://doi.org/10.1016/j.desal.2015.03.001.

[4] J. H. Jhaveri and Z. V. P. Murthy, "A comprehensive review on anti-fouling nanocomposite membranes for pressure driven membrane separation processes," *Desalination*, vol. 379, pp. 137–154, Feb. 2016, https://doi.org/10.1016/j.desal.2015.11.009.

[5] D. L. Gin and R. D. Noble, "Designing the Next Generation of Chemical Separation Membranes," *Science*, vol. 332, no. 6030, pp. 674–676, May 2011, https://doi.org/10.1126/science.1203771.

[6] A. Rahimpour, M. Jahanshahi, S. Khalili, A. Mollahosseini, A. Zirepour, and B. Rajaeian, "Novel functionalized carbon nanotubes for improving the surface properties and performance of polyethersulfone (PES) membrane," *Desalination*, vol. 286, pp. 99–107, Feb. 2012, https://doi.org/10.1016/j.desal.2011.10.039.

[7] M. B. Alkindy, V. Naddeo, F. Banat, and S. W. Hasan, "Synthesis of polyethersulfone (PES)/GO-SiO2 mixed matrix membranes for oily wastewater treatment," *Water Sci. Technol.*, vol. 81, no. 7, pp. 1354–1364, Apr. 2020, https://doi.org/10.2166/wst.2019.347.

[8] T. Remiš, P. Bělský, S. M. Andersen, M. Tomáš, J. Kadlec, and T. Kovářík, "Preparation and Characterization of Poly(Vinyl Alcohol) (PVA)/SiO $_2$, PVA/Sulfosuccinic Acid (SSA) and PVA/SiO $_2$ /SSA Membranes: A Comparative Study," *J. Macromol. Sci. Part B*, vol. 59, no. 3, pp. 157–181, Mar. 2020, https://doi.org/10.1080/00222348.2019.1697023.

[9] Z. Peng and Y. Shen, "Study on Biological Safety of Polyvinyl Alcohol/Collagen Hydrogel as Tissue Substitute (I)," *Polym.-Plast. Technol. Eng.*, vol. 50, no. 3, pp. 245–250, Jan. 2011, https://doi.org/10.1080/03602559.2010.531438.

[10] T. Malik *et al.*, "Design and synthesis of polymeric membranes using water-soluble pore formers: an overview," *Polym. Bull.*, vol. 76, no. 9, pp. 4879–4901, Sep. 2019, https://doi.org/10.1007/s00289-018-2616-3.

[11] T. A. Otitoju, M. Ahmadipour, S. Li, N. F. Shoparwe, L. X. Jie, and A. L. Owolabi, "Influence of nanoparticle type on the performance of nanocomposite membranes for wastewater treatment," *J. Water Process Eng.*, vol. 36, p. 101356, Aug. 2020, https://doi.org/10.1016/j.jwpe.2020.101356.

[12] C. Kahrs and J. Schwellenbach, "Membrane formation via non-solvent induced phase separation using sustainable solvents: A comparative study," *Polymer*, vol. 186, p. 122071, Jan. 2020, https://doi.org/10.1016/j.polymer.2019.122071.

[13] A. Asad, D. Sameoto, and M. Sadrzadeh, "Overview of membrane technology," in *Nanocomposite Membranes for Water and Gas Separation*, Elsevier, 2020, pp. 1–28. https://doi.org/10.1016/B978-0-12-816710-6.00001-8.

[14] S. Amiri, A. Asghari, V. Vatanpour, and M. Rajabi, "Fabrication of chitosan-aminopropylsilane graphene oxide nanocomposite hydrogel embedded PES membrane for improved filtration performance and lead separation," *J. Environ. Manage.*, vol. 294, p. 112918, Sep. 2021, https://doi.org/10.1016/j.jenvman.2021.112918.

[15] D. Sun, D. Yue, B. Li, Z. Zheng, and X. Meng, "Preparation and performance of the novel PVDF ultrafiltration membranes blending with PVA modified SiO $_2$ hydrophilic nanoparticles: novel PVDF ultrafiltration membranes," *Polym. Eng. Sci.*, vol. 59, no. S1, pp. E412–E421, Jan. 2019, https://doi.org/10.1002/pen.25002.

[16] M. Farnam, H. Mukhtar, and A. M. Shariff, "An investigation of blended polymeric membranes and their gas separation performance," *RSC Adv.*, vol. 6, no. 104, pp. 102671–102679, 2016, https://doi.org/10.1039/C6RA21574B.

[17] K. Shameli *et al.*, "Synthesis and Characterization of Polyethylene Glycol Mediated Silver Nanoparticles by the Green Method," *Int. J. Mol. Sci.*, vol. 13, no. 6, pp. 6639–6650, May 2012, https://doi.org/10.3390/ijms13066639.

[18] M. A. Ramlli, M. A. Maksud, and M. I. N. Isa, "Characterization of polyethylene glycol plasticized carboxymethyl cellulose-ammonium fluoride solid biopolymer electrolytes," in Renewable Energy Technology and Innovation For Sustainable Development: Proceedings of the International Tropical Renewable Energy Conference (i-TREC) 2016, (Bogor, Indonesia), 2017, p. 020001. https://doi.org/10.1063/1.4979217.

[19] H. A. Mannan, H. Mukhtar, T. Murugesan, R. Nasir, D. F. Mohshim, and A. Mushtaq, "Recent Applications of Polymer Blends in Gas Separation Membranes," *Chem. Eng. Technol.*, vol. 36, no. 11, pp. 1838–1846, Nov. 2013, https://doi.org/10.1002/ceat.201300342.

[20] J. Shen, H. Ruan, L. Wu, and C. Gao, "Preparation and characterization of PES–SiO2 organic–inorganic composite ultrafiltration membrane for raw water pretreatment," *Chem. Eng. J.*, vol. 168, no. 3, pp. 1272–1278, Apr. 2011, https://doi.org/10.1016/j.cej.2011.02.039.

[21] A. Asad, M. Sadrzadeh, and D. Sameoto, "Direct Micropatterning of Phase Separation Membranes Using Hydrogel Soft Lithography," *Adv. Mater. Technol.*, vol. 4, no. 7, p. 1800384, Jul. 2019, https://doi.org/10.1002/admt.201800384.

[22] Q. Wang, S. Zhang, X. Ji, and F. Ran, "High rejection performance ultrafiltration membrane with ultrathin dense layer fabricated by the movement and dissolution of metal–organic frameworks," *New J. Chem.*, vol. 44, no. 32, pp. 13745–13754, 2020, https://doi.org/10.1039/D0NJ02700F.

[23] F. Liu, "Hydrophilic Membrane," in *Encyclopedia of Membranes*, E. Drioli and L. Giorno, Eds., Berlin, Heidelberg: Springer Berlin Heidelberg, 2016, pp. 1000–1000. https://doi.org/10.1007/978-3-662-44324-8_1676.

[24] J. Babu and Z. V. P. Murthy, "Treatment of textile dyes containing wastewaters with PES/PVA thin film composite nanofiltration membranes," *Sep. Purif. Technol.*, vol. 183, pp. 66–72, Aug. 2017, https://doi.org/10.1016/j.seppur.2017.04.002.

[25] H. S. Erkan, N. B. Turan, and G. Ö. Engin, "Membrane Bioreactors for Wastewater Treatment," in *Comprehensive Analytical Chemistry*, vol. 81, pp. 151–200, 2018 https://doi.org/10.1016/bs.coac.2018.02.002.

[26] J. Shen, H. Ruan, L. Wu, and C. Gao, "Preparation and characterization of PES–SiO2 organic–inorganic composite ultrafiltration membrane for raw water pretreatment," *Chem. Eng. J.*, vol. 168, no. 3, pp. 1272–1278, Apr. 2011, https://doi.org/10.1016/j.cej.2011.02.039.

[27] A. S. Ismail, S. M. Tawfik, A. H. Mady, and Y.-I. Lee, "Preparation, Properties, and Microbial Impact of Tungsten (VI) Oxide and Zinc (II) Oxide Nanoparticles Enriched Polyethylene Sebacate Nanocomposites," *Polymers*, vol. 13, no. 5, p. 718, Feb. 2021, https://doi.org/10.3390/polym13050718.

[28] Y. Z. N. Htwe and M. Mariatti, "Fabrication and characterization of silver nanoparticles/PVA composites for flexible electronic application," in 3rd International Postgraduate Conference on Materials, Minerals & Polymer (MAMIP) 2019, (Penang, Malaysia), 2020, p. 020046. https://doi.org/10.1063/5.0016135.

[29] X. Gong, C. Y. Tang, L. Pan, Z. Hao, and C. P. Tsui, "Characterization of poly(vinyl alcohol) (PVA)/ZnO nanocomposites prepared by a one-pot method," *Compos. Part B Eng.*, vol. 60, pp. 144–149, Apr. 2014, https://doi.org/10.1016/j.compositesb.2013.12.045.

[30] M. B. Ahmad, M. Y. Tay, K. Shameli, M. Z. Hussein, and J. J. Lim, "Green Synthesis and Characterization of Silver/Chitosan/Polyethylene Glycol Nanocomposites without any Reducing Agent," *Int. J. Mol. Sci.*, vol. 12, no. 8, pp. 4872–4884, Aug. 2011, https://doi.org/10.3390/ijms12084872.

[31] J. Widakdo, N. Istikhomah, A. Rifianto, E. Suharyadi, T. Kato, and S. Iwata, "Crystal Structures and Magnetic Properties of Polyethylene Glycol (PEG-4000) Encapsulated $Zn_{0.5}Ni_{0.5}Fe_2O_4$ Magnetic Nanoparticles," *J. Phys. Conf. Ser.*, vol. 1011, p. 012068, Apr. 2018, https://doi.org/10.1088/1742-6596/1011/1/012068.

[32] X. Hong, L. Zou, J. Zhao, C. Li, and L. Cong, "Dry-wet spinning of PVA fiber with high strength and high Young's modulus," *IOP Conf. Ser. Mater. Sci. Eng.*, vol. 439, p. 042011, Nov. 2018, https://doi.org/10.1088/1757-899X/439/4/042011.

[33] H. Li, Y. Guo, J. Robertson, and Y. Okuno, "*Ab-initio* simulations of higher Miller index Si:SiO2 interfaces for fin field effect transistor and nanowire transistors," *J. Appl. Phys.*, vol. 119, no. 5, p. 054103, Feb. 2016, https://doi.org/10.1063/1.4941272.

[34] S. M. Ulfa, R. F. Ohorella, and C. W. Astutik, "Sequential Condensation and Hydrodeoxygenation Reaction of Furfural-Acetone Adduct over Mix Catalysts Ni/SiO_2 and Cu/SiO_2 in Water," *Indones. J. Chem.*, vol. 18, no. 2, p. 250, May 2018, https://doi.org/10.22146/ijc.26736.

[35] Y. Alqaheem and A. A. Alomair, "Microscopy and Spectroscopy Techniques for Characterization of Polymeric Membranes," *Membranes*, vol. 10, no. 2, p. 33, Feb. 2020, https://doi.org/10.3390/membranes10020033.

[36] D. Sun, D. Yue, B. Li, Z. Zheng, and X. Meng, "Preparation and performance of the novel PVDF ultrafiltration membranes blending with PVA modified SiO_2 hydrophilic nanoparticles: novel PVDF ultrafiltration membranes," *Polym. Eng. Sci.*, vol. 59, no. S1, pp. E412–E421, Jan. 2019, https://doi.org/10.1002/pen.25002.

[37] H. El-Didamony, E. El-Fadaly, A. A. Amer, and I. H. Abazeed, "Synthesis and characterization of low cost nanosilica from sodium silicate solution and their applications in ceramic engobes," *Bol. Soc. Esp. Cerámica Vidr.*, vol. 59, no. 1, pp. 31–43, Jan. 2020, https://doi.org/ 10.1016/j.bsecv.2019.06.004.

[38] K. Shameli *et al.*, "Synthesis and Characterization of Polyethylene Glycol Mediated Silver Nanoparticles by the Green Method," *Int. J. Mol. Sci.*, vol. 13, no. 6, pp. 6639–6650, May 2012, https://doi.org/10.3390/ijms13066639.

[39] S. Amiri, A. Asghari, V. Vatanpour, and M. Rajabi, "Fabrication of chitosan-aminopropylsilane graphene oxide nanocomposite hydrogel embedded PES membrane for improved filtration performance and lead separation," *J. Environ. Manage.*, vol. 294, p. 112918, Sep. 2021, https://doi.org/10.1016/j.jenvman.2021.112918.

[40] A. B. D. Nandiyanto, R. Oktiani, and R. Ragadhita, "How to Read and Interpret FTIR Spectroscope of Organic Material," *Indones. J. Sci. Technol.*, vol. 4, no. 1, p. 97, Mar. 2019, https://doi.org/10.17509/ijost.v4i1.15806.